On the Nature of Reduced States in Titanium Dioxide As Monitored by Electron Paramagnetic Resonance. I: The Anatase Case

UNIVERSITÀ DEGLI STUDI DI TORINO

On the Nature of Reduced States in Titanium Dioxide as Monitored by Electron Paramagnetic Resonance. I: The Anatase case.

Stefano Livraghi, Mario Chiesa, Maria Cristina Paganini, Elio Giamello*.

Dipartimento di Chimica IFM, Università di Torino and NIS, Nanostructured Interfaces and Surfaces Centre of Excellence, Via P. Giuria 7, I - 10125 Torino, Italy

**corresponding Author*

elio.giamello@unito.it

Abstract

A systematic analysis of the reduced states in the titanium dioxide matrix (anatase polymorph) has been performed coupling the classic Continuous Wave Electron Paramagnetic Resonance (CW-EPR) with advanced pulse-EPR techniques and introducing the ^{17}O magnetic isotope into the solid. Reduced states were originated in various ways including valence induction via aliovalent elements (F, Nb) and reducing treatments of the bare oxide including surface reaction with reducing agents (H, Na) and thermal annealing under vacuum with consequent oxygen depletion. Two main paramagnetic species were identified via EPR both amenable to Ti^{3+} ions. The former (EPR signal A: axial symmetry with $g_{\|}$=1.962 and $g_{\perp}$= 1.992) is observed in all case and has been conclusively assigned to reduced Ti^{3+} centres in regular lattice sites of the anatase matrix; the second (signal B: broad line centred at g= 1.93) is present only in reduced materials and is assigned, on the basis of the analysis of the hyperfine interaction of the centres with ^{17}O labelled ions in its environment, to a collection of slightly different Ti^{3+} centres located at the surface, or in the subsurface region. The hyperfine interaction of the lattice Ti^{3+} centres corresponding to signal A with ^{17}O was investigated by HYSCORE spectroscopy and resulted in a maximum hf coupling of the order of 2 MHz which is nearly one order of magnitude less than that recently measured for reduced centres in rutile. This surprising result suggests that excess electrons corresponding to signal A are not localized on a single ion but are likely delocalized on several analogous titanium lattice ions. This result (compatible with recent theoretical calculations) has relevance with respect to the living debate about localisation and delocalisation of electrons in titania which has been based, up to now, on conflicting evidences.

1. **Introduction**

Titanium dioxide is a strategic material produced in huge amounts for classical applications as a cheap white pigment. However the importance of this solid, in future perspective, mainly relies on its photochemical and photophysical properties[1]. Titanium dioxide in fact is an efficient photocatalyst in several reactions for environmental remediation[2] and, since the fundamental discovery of water photosplitting in 1972[3], it can also be considered as a system of interest for applications in the field of energy production. More recently titanium dioxide has found new employments as biocide[4] in odour control[5] and, under the form of a ultrathin film, as a superhydrophilic antifogging agent[6]. Also important is the use of titanium dioxide in dye-sensitized solar cells[7] a class of photovoltaic devices for solar light energy harvesting.

Titanium dioxide belongs to the class of reducible oxides as it easily looses oxygen with formation of oxygen vacancies and, in parallel, of excess electrons which are stabilized into the reduced solid. The formation of charge carriers is also typical of the phenomena described above (photocatalysis, photovoltaic systems) which always start with a photoinduced charge separation[8-10] and the migration of the carriers (electrons and holes) into the solid. The phenomena of charge transport, stabilisation, recombination and reactivity is therefore of vital importance to understand the properties of titanium dioxide and to develop strategies to control these properties (for example to reduce the undesired charge recombination in photocatalytic phenomena).

Due to the importance of titanium dioxide and to the many still open problems concerning this matrix, it is not surprising that TiO_2 has been the object of thousands of investigations in recent years. Particularly broad is the range of investigations available in the surface science of single-crystalline systems which make of TiO_2 the most investigated oxide in this area[11]. Very intense is, in parallel, the computational activity aimed to explore the structure of the surface[12,13] and the phenomena of charge transport[14] and stabilisation[15]. The two most important polymorphs of titanium dioxide are rutile and anatase. While rutile is the most stable thermodynamic phase, anatase is certainly more important under the point of view of the photochemical applications. Paradoxically rutile has long been the most investigated phase by the surface scientist and anatase has been more considered in characterisation activities using polycrystalline solids, due to its peculiar photochemical properties.

The present paper is the first of a short series aiming to rationalise the features of excess electron centres in titanium dioxide exploiting the potential of the Electron Paramagnetic Resonance (EPR) techniques. As already discussed, this topics is of vital importance in nearly all the phenomena concerning TiO_2 since excess electron centres or reduced species, usually interpreted as Ti^{3+} ions,

are formed either by small stoichiometric variations in the composition of this easily reducible oxide or by chemical reaction with electron donors (hydrogen, alkaline metals). In the former case loss of one lattice oxygen causes the formation, beside the oxygen vacancy, of two excess electrons in the solid according to the following notation:

$$O^{2-} + 2Ti^{4+} \rightarrow \frac{1}{2} O_2 + V_O^{\cdot\cdot} + 2\ Ti^{3+} \qquad (1)$$

where the oxygen vacancy is indicated using the Kröger and Vink notation and is supposed to be empty, while the excess electrons are stabilized by the solid under the form of Ti^{3+} (*vide infra*). By the way also electrons resulting from charge separation in the bare, irradiated solid are stabilized as Ti^{3+} [16,17].

There is a large bulk of evidence about the presence of Ti^{3+} in reduced or in irradiated TiO_2 which derive from photoelectron spectroscopy[18], polarized optical spectroscopy[19], EELS spectroscopy [20] and Electron Paramagnetic Resonance [16-21]. However, several questions concerning the true nature of the reduced centres remain open, in particular those related to the location of Ti^{3+} ions (lattice or interstitial position)[22], the correlation (if any) of these ions with the oxygen vacancies in reduced solids, the surface or bulk nature of the centres. Beside this typical structural problems at least another fundamental question remains open which is related to the nature of the electronic states associated to the defects whose wave function can be seen as localized on a single titanium ion (producing an intra band gap state) or delocalized on several of them as also suggested by recent resonant photoelectron diffraction experiments[23]. This intrinsically complex problem is further complicated by two factors. The former one is the role of temperature which, beyond a certain limit, induces charge transport phenomena based on the polaron hopping mechanism[21a,24] while the second one is the lack of a clear cut picture of the system deriving from theoretical modelling. The theoretical descriptions of reduced titanium oxide, in fact, are much affected by the choice of the method. Furthermore, as clearly shown in a recent feature article[15c], a given theoretical method often gives rise to fully localized and highly delocalized solutions having extremely close energy values, thus seriously limiting the possibility of a clear indication derived from theory .

To use EPR in the investigation of reduced states of titanium dioxide appears as a natural choice due to the high capability of the technique in describing paramagnetic defects in solids[25] . The technique has been actually exploited, on one hand, in several studies of rutile single crystals[21a,c, 26-28] mainly aimed to understand the symmetry of Ti^{3+} centres or the role of impurities. On the other hand the investigations nowadays available of polycrystalline systems are mainly related to phenomenological aspects (formation of reduced Ti^{3+} centres in various conditions, reactivity with adsorbates etc.) rather than to a systematic analysis of the nature of the centres themselves. This limitation is caused essentially by the fact that the concentration of magnetic isotopes in TiO_2 (^{47}Ti,

^{49}Ti,^{17}O) is too low and prevents the observation of the spectral structures related to the hyperfine interactions which are essential to monitor the localization degree of the wavefunction. The information usually derived by EPR on Ti^{3+} is limited thus to that based on the *g* tensor. This parameter is sensitive to the symmetry of the system, but less sensitive to electron delocalization. This limitation is probably the reason of the lack of a thorough, EPR based, analysis of the various types of Ti^{3+} centres present in titanium dioxide which is indeed the subject of the present work. In the first part of the paper we will report and discuss Ti^{3+} EPR spectra obtained in various conditions analysing, by the classic continuous wave technique (CW-EPR) samples constituted by the anatase polymorph. Excess electrons have been introduced in the solid by various methods including valence induction, surface reactivity and oxygen depletion and different types of signal have been conclusively classified. Furthermore the enrichment of the matrix with the ^{17}O isotope has been performed and the interaction between the unpaired electron and the surrounding oxygen ions will be described. This interaction is extremely weak and Pulse-EPR techniques are necessary to gain information on the isotopically enriched oxide.

2. Experimental

Samples preparation. Pure TiO_2 was prepared by Chemical Vapour Deposition (CVD) by oxidation of Titanium isopropoxide in a home made flow reactor based on a similar apparatus developed by Prof. O. Diwald[29]. The apparatus contains a first section where the evaporation of the titanium precursor occurs followed by transport of the precursor in the reaction section using Argon as carrier gas. In this second section the titanium compound reacts with pure O_2 at high temperature. Gas flows were 800 SCCM and 200 SCCM for Ar and O_2 respectively. Evaporation temperature in section 1 and reaction temperature in section 2 of the apparatus were 573 K and 1023K respectively.

The sol-gel method was used to prepare X-doped TiO_2 systems with X= F^-, Nb^{5+}. The preparation was carried out by the reaction of a solution of titanium (IV) isopropoxide in isopropylic alcohol (molar ratio 1: 4) with water (molar ratio between alcohol and water 1:10) performed under constant stirring at room temperature. The gel so obtained was aged overnight at room temperature to ensure the conclusion of the hydrolysis and was subsequently dried at 343 K. The dried material was heated at 773 K in air (heating rate 10 K/min.) for 1 h. To prepare fluorine doped materials (hereafter F-TiO_2) an hydrofluoric acid solution (2M) was employed instead of pure water. Niobium pentacloride was adopted to obtain Nb-TiO_2.

^{17}Oxygen enrichment. Two different approaches were adopted to obtain ^{17}O enriched TiO_2 i.e. $^{17}O_2$ reaction from gas phase with a thermally annealed solid and direct synthesis of the oxide by hydrolysis of $TiCl_4$ employing ^{17}O enriched water.

As to the first method, pure TiO_2 was heated in dynamic vacuum for 30 minutes (residual $P < 10^{-3}$ mbar) at 773K and subsequently oxidized at the same temperature in 10 mbar of ^{17}O enriched O_2 (Aldrich, enrichment =90%) for 1 h.

Alternatively the solid was prepared by hydrolysis of $TiCl_4$ (Aldrich 99.999%) with a stoichiometric amount of ^{17}O isotopically enriched water (40% ^{17}O enrichment supplied by Icon Services New Jersey) under N_2 flow. In a typical synthesis H_2O was slowly dripped onto $TiCl_4$ in an apparatus connected to a trap filled with NaOH in order to neutralize the hydrochloric acid formed during the reaction. After hydrolysis the powder was kept under N_2 flow for 2 hours. The solid so obtained was aged overnight at room temperature to ensure the conclusion of the hydrolysis and was subsequently dried at 343 K. The dried material was heated in a closed tube at 773 K (heating rate 10 K/min.) in 10 mbar of ^{17}O enriched O_2 (90%) for 1 h.

^{17}O enriched F-TiO_2 was prepared by hydrolysis of a mixture made up by 80mol% of $TiCl_4$ and 20mol% of TiF_4 with the same procedure reported above.

Atomic hydrogen used in some experiment was generated in situ by means of a glow microwave discharge operating at 2.45 GHz.

Experimental techniques. Electron Paramagnetic Resonance (EPR) spectra were run on a X-band CW-EPR Bruker EMX spectrometer equipped with a cylindrical cavity operating at 100 KHz field modulation. Irradiation experiments were performed irradiating the samples with a 500 W mercury/xenon lamp (Oriel instruments) equipped with a IR water filter.

Pulse EPR experiments were performed on an ELEXYS 580 Bruker spectrometer (microwave frequency of 9.76 GHz) equipped with a liquid-helium cryostat from Oxford Inc. The magnetic field was measured by means of a Bruker ER035M NMR gaussmeter.

Electron-spin-echo (ESE) detected EPR. The experiments were carried out with the pulse sequence: $\pi/2 - \tau - \pi - \tau$–echo, with mw pulse lengths $t_{\pi/2}$ = 16 ns and t_π = 32 ns and a τ value of 200 ns.

Three-pulse ESEEM (electron spin echo envelope modulation). Experiments were carried out using the pulse sequence $\pi/2 - \tau - \pi/2 - T - \pi/2 - \tau$ –echo with mw pulses of length $t_{\pi/2}$ = 16 ns, a starting time T_0=96 ns and a time increment ΔT=16 ns (512 intervals).

Hyperfine Sublevel Correlation (HYSCORE) [30] experiments were carried out with the pulse sequence $\pi/2 - \tau - \pi/2 - t_1 - \pi - t_2 - \pi/2 - \tau$-echo with mw pulse length $t_{\pi/2}$ = 16 ns and t_π = 16 ns. The time intervals t_1 and t_2 were varied in steps of 16 ns starting from 96 ns to 3288 ns. Spectra were recorded at two different τ values (112 ns and 160 ns). An eight-step phase cycle was used for

eliminating unwanted echoes. The time traces of the HYSCORE spectra were baseline corrected with a third-order polynomial, apodized with a Hamming window and zero filled. After two-dimensional Fourier transformation, the absolute value spectra were calculated. The spectra were added for the different τ values in order to eliminate blind-spot effects. The HYSCORE spectra were simulated using the Easyspin program. [31]

3. Results and discussion.

3.1. Ti^{3+} in anatase generated by valence induction.

The alteration of the ionic charge caused by the presence of an aliovalent element into an ionic lattice is a well known phenomenon in solid state chemistry. Ti^{3+} ions in anatase have been generated diluting either an anion (F^-) or a cation (Nb^{5+}) in the matrix during the synthesis. All the two dopants bear one extra electron with respect to the stoichiometry of titanium dioxide. The doped samples show the XRD pattern typical of anatase and no evidence of a different phase is present (the diffractograms, not reported here for sake of brevity, are available as supplementary materials). Both powders are white and no appreciable optical absorption is observed in the visible range.

Since all the mentioned dopants occupies regular lattice sites, the solid compensates the valence alteration producing in both cases an amount of Ti^{3+} corresponding to that of the dopant. The two solids can be written respectively as $Ti^{4+}_{(1-x)}\ Ti^{3+}_{x}\ O^{2-}_{(2-x)}\ F^{-}_{x}$ and $Ti^{4+}_{(1-x)}\ Nb^{5+}_{x}\ Ti^{3+}_{x}\ O^{2-}_{2}$. Niobium doping of titania (mainly rutile) has been previously investigated by EPR in powders by Valigi et al.[32] and by Kiwi et al[33] while fluorine doping of anatase was reported by different Authors[34,35] including some of us[36]. The two doped and fully oxidized samples exhibits a sharp and apparently axial EPR signal unambiguously amenable to Ti^{3+} ions. The spectra obtained by CW-EPR in X band (9.5 GHz) are reported in Fig 1 (a and b) and are, apart some small difference in the linewidth, practically superimposable. In order to better characterize the doped sample, EPR spectra of F doped TiO_2 were recorded at W band frequency (95 GHz). Under these circumstances a much higher resolution is achieved, allowing to better resolve the *g* tensor components of the spectrum. The spectrum recorded at W band at 10 K is shown in Figure 1c and confirms the axial nature of the signal observed at X band frequency ($g_{zz}= g_{\|}=1.962$ and $g_{xx}=g_{yy}=g_{\perp}= 1.992$). All samples giving rise to the spectra in Fig. 1 have been calcined in air at 673K and the spectral features are stable under a ordinary atmosphere. In other words the Ti^{3+} ions are typical features of the doped system whose origin is due to the compensation of the extracharge carried by the dopant and not to a partial reduction of the solid. The features of signal A appear unperturbed when the signal is recorded at

77K under a layer of physisorbed oxygen. This indicates that no appreciable dipolar interaction occurs between Ti^{3+} ions and O_2 and that the reduced ions are not located at the surface.

As it will be better detailed in Section 3.4 signal A has to be assigned to Ti^{3+} ions in regular position of the anatase lattice. The concentration of F^- (hence Ti^{3+}) in the solid can be tuned using different HF solution during the preparation. In the case of the present results the loading of F^-, measured by EPR via spin counting of Ti^{3+}, is about 13 ppm.

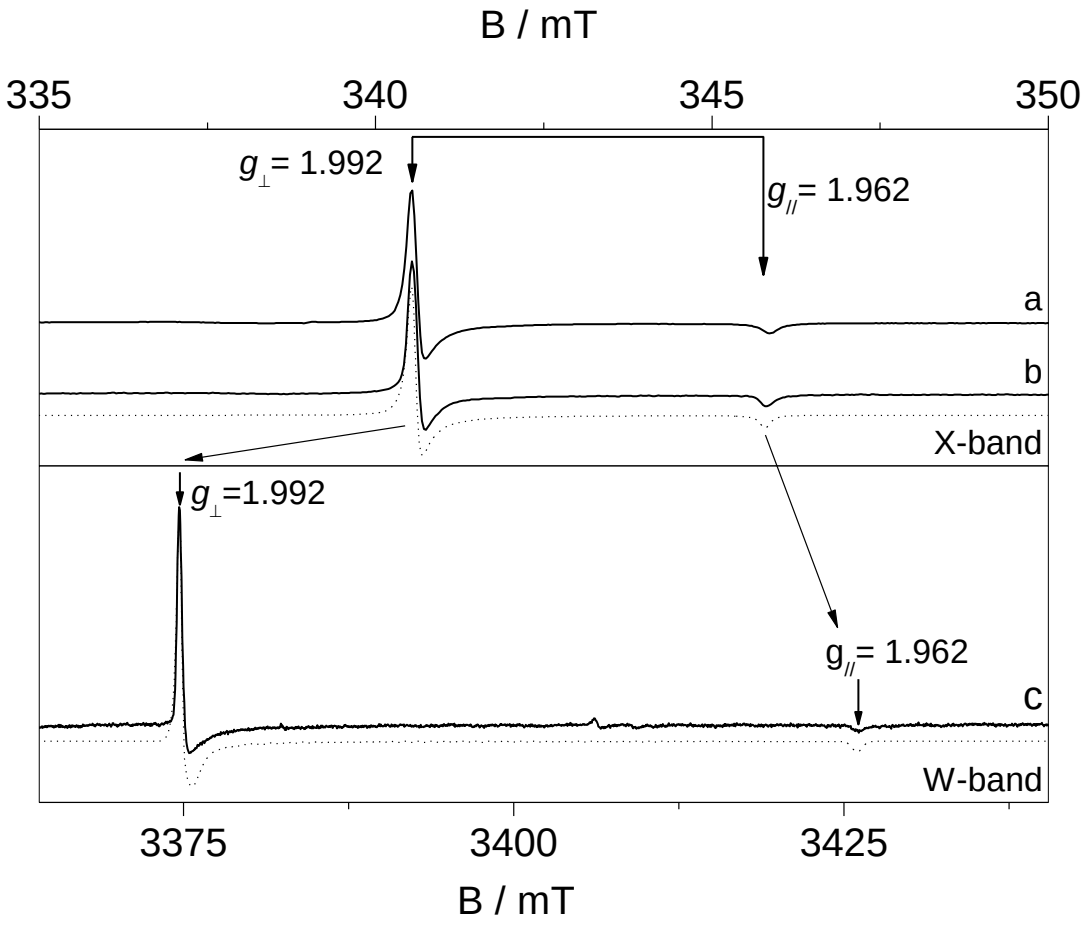

Figure 1. X-band CW-EPR spectra of Nb-TiO_2 (a) and F-TiO_2 (b); W-band spectrum of F-TiO_2 (c). Spectra recorded at 77K. The dotted line are computer simulations of the spectra.

3.2. Reduced states generated by reaction with electron donors.

Figure 2 reports the spectra obtained by surface reaction of bare TiO_2 with an electron donor. In the two former cases (Fig.2a and 2b) the electron donor is atomic hydrogen which is generated either by microwave discharge in H_2 with direct formation of H atoms in the atmosphere (Fig. 2b) or by UV irradiation again in H_2 atmosphere (Fig.2a). In this case the UV light induces the well known charge separation with formation of an electron and a hole. As shown by Diwald and coworkers the

hole, once migrated at the surface, reacts with molecular hydrogen to give an hydroxyl group and an H atom which ionizes injecting an electron in the solid ($2O^{2-}_{surf} + h^+ + H_2 \rightarrow OH^-_{surf} + O^{2-}_{surf} + H \rightarrow 2OH^-_{surf} + e^-$).[37] In the case of both Fig.s 2a and 2b the reducing agent is thus atomic hydrogen. The spectrum in Fig 2c was obtained by contacting the anatase surface with sodium vapors producing Na^+ ions and electrons while the last spectrum (2d) has been recorded after a mild thermal reduction by annealing under vacuo at 570K and is reported here for comparison being discussed in detail in the next Section. The spectra described above are very similar one to the other. In particular those in Fig. 2a and 2b are almost coincident. The spectra in Fig. 2, though more complex of those in Fig.1, include the features of species A which are again reported, for sake of comparison, in Fig.2e. These observations indicate therefore that one of the consequences of the direct injection of electrons in the solid through its surface is the formation of a reduced centre at a regular lattice site.

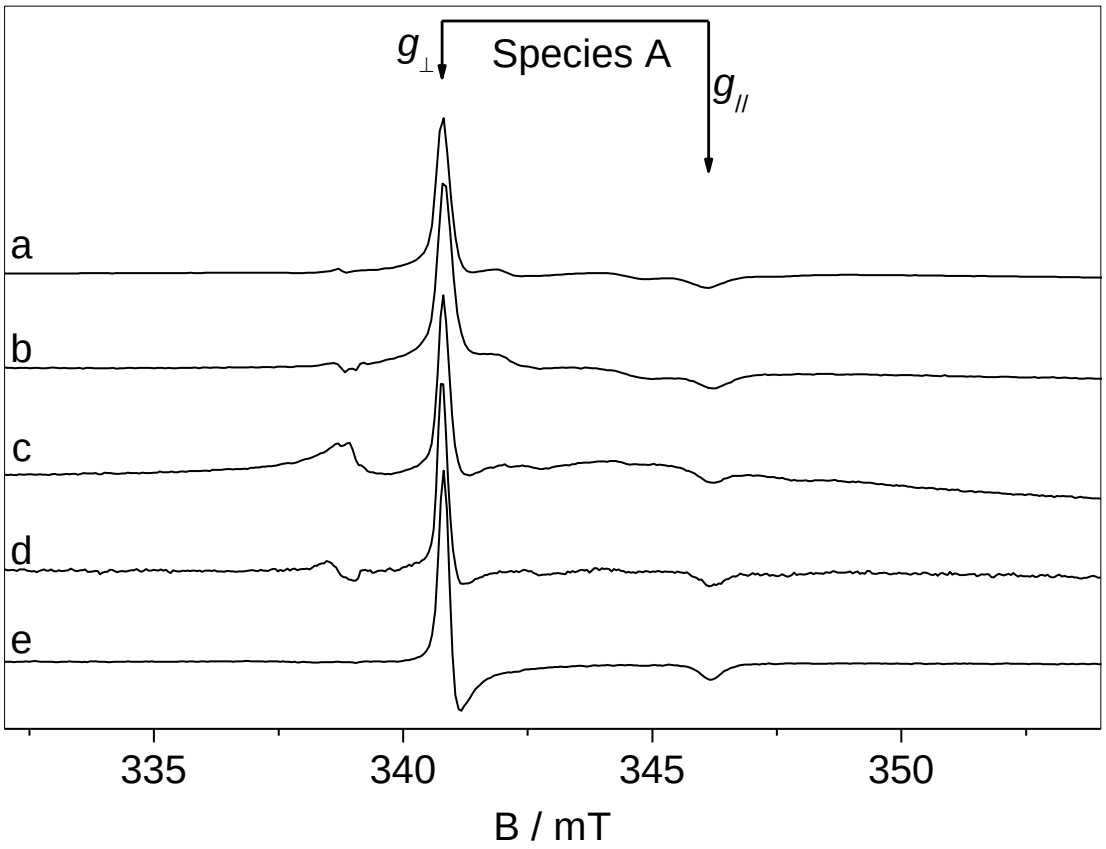

Figure 2 CW-EPR spectra in X band of a) UV-irradiated anatase in hydrogen atmosphere, b) anatase contacted with atomic hydrogen, c) anatase treated with Na vapors, d) anatase annealed in vacuo at 570K, e) Nb-TiO_2 (for comparison)

The spectra in Fig.2 (a-d) however are made up by more than one single signal as indicated by the profile around the perpendicular component of signal A which is perturbed by the overlap with some other signal (very minor features between $g_{\|}$ and $g_{\perp}$ of signal A will be discussed later on in terms of signal C) and, more important, by the base line trend which seems suggesting the existence of a broad signal at high field. This impression is confirmed by the elctron spin echo (ESE) - detected EPR spectra reported in Fig. 3 and related to thermally reduced (a) UV irradiated under H_2 (b) and F doped (c) anatase samples. The ESE detected EPR spectrum corresponds to the absorption of the conventional CW-EPR spectrum and is more effective in detecting broad signals, which become hardly observed in the derivative spectrum. Fig.3 clearly indicates that species A, apparently dominant in CW-EPR spectra of Fig. 2, is actually only a minor fraction of the whole reduced centers generated by either thermal reduction or UV irradiation under H_2. The most important species, in quantitative terms corresponds to a broad unstructured signal (signal B) centred at approximately g = 1.93 and extending over approximately 35 mT. The large linewidth corresponding to species B could in principle be ascribed to either fast relaxation pathways or strain effects associated to a substantial heterogeneity of the paramagnetic centres. The decay of the 2-pulse ESE time traces of both species A and B could be fitted with a bi-exponential decay with a dominant contribution of a short T_m value in the order of 250-350 ns and a smaller fraction of a long T_m value in the order of 4-11 μs. This indicates that the two centers have similar relaxation characteristics and leaves as a most likely source of broadening for species B strain effects associated to the presence of different sites with slightly different local environment and therefore slightly different EPR parameters. It is worth noticing that signal B is totally absent in the spectrum of F-TiO_2 (1a, 2a, 3c) confirming that this signal is related to the perturbations caused by thermal or chemical treatments to the solid.

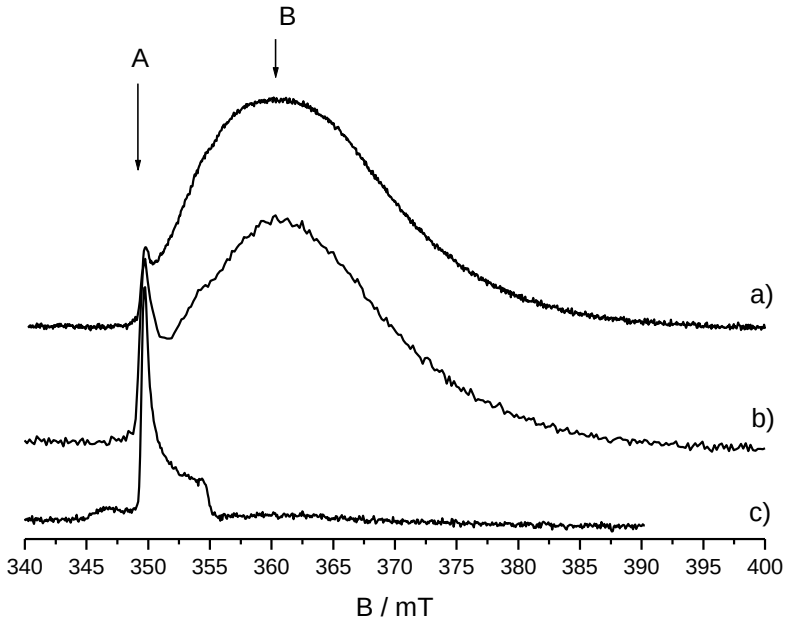

Figure 3 ESE-detected EPR spectra of a) CVD anatase thermally reduced by annealing in vacuo at 570K; b) CVD anatase UV irradiated under hydrogen; c) F doped anatase . All spectra were recorded at 10 K, and the same recording conditions were taken. The spectra were then normalized.

.

Taking into account the origin of the spectra in Fig. 2a-d and 3a-b (surface reaction with electron donors or reduction by annealing) it seems clear that the origin of signal B has to be ascribed to a collection of surface and sub-surface reduced Ti^{3+} centres whose heterogeneity derives from several factors including the local coordination of the ion, the symmetry of the particular crystal face hosting the reduced ion, the presence of OH groups (or Na^{+} ions) formed upon reaction and located in the vicinity of the paramagnetic center. It is worth mentioning that, in a recent paper based on the analysis of TiO_2-ZrO_2 solid solutions[38] it was possible to show, due to the simultaneous presence of two distinct cations in the solid, that the broad EPR signal between g =1.977 and g = 1.908 strictly similar to the one here reported (species B for TiO_2) after a reducing treatment is indeed due to Ti^{3+} ions present at the surface.

To substantiate this assignment ad hoc experiments have been carried out introducing ^{17}O enriched O_2 into the solid. A reduced anatase sample (oxygen depleted) was reoxidized using $^{17}O_2$ (99%). In this way it is assumed that O_2 molecules dissociate, filling the surface vacancies generated during the thermal treatment [39, 40] The colourless, diamagnetic sample was then reduced by UV irradiation under H_2, resulting in the typical EPR spectrum shown in Fig 4a, very similar to that reported in Fig.s 3 a and b.

3-Pulse ESEEM spectra where then taken at magnetic field settings corresponding to species A and B (indicated by the arrows in Figure 4a) respectively. The 3P-ESEEM measurements of ^{17}O

modulation of the two different Ti^{3+} species produced by UV irradiation under H_2 provide convincing evidence for the surface nature of species B. The three-pulse ESEEM patterns recorded by selecting the interpulse time $\tau = 0.25$ μs at field positions corresponding to species A and B are shown in Figure 4b and 4d respectively, while the corresponding Fourier transform is shown in Figure 4c and 4e. Despite the echo intensity at positions 1 and 2 is practically the same, the ^{17}O modulation depth is much stronger in the case of species B, indicating a higher number of ^{17}O nuclei interacting with the Ti^{3+} centres. This can be explained considering that the ^{17}O enrichment is limited to the surface and subsurface region of the sample. The shallow modulations associated to species A can be explained considering that at this field positions contributions of species B (see Fig 4.a) are also present. The Fourier transform spectrum of the 3P ESEEM spectrum associated to species B (Fig 4e) consists of a single sharp peak centred at about 2.1 MHz corresponding to the ^{17}O Larmor frequency, suggesting that the observed signal is not associated to directly coordinated oxygen nuclei or that the unpaired electron wave function encompasses several lattice sites. (vide infra). The described experiment thus provides strong evidence that the broad signal generated upon reduction in the presence of H_2 or upon thermal annealing is indeed due to surface or subsurface species.

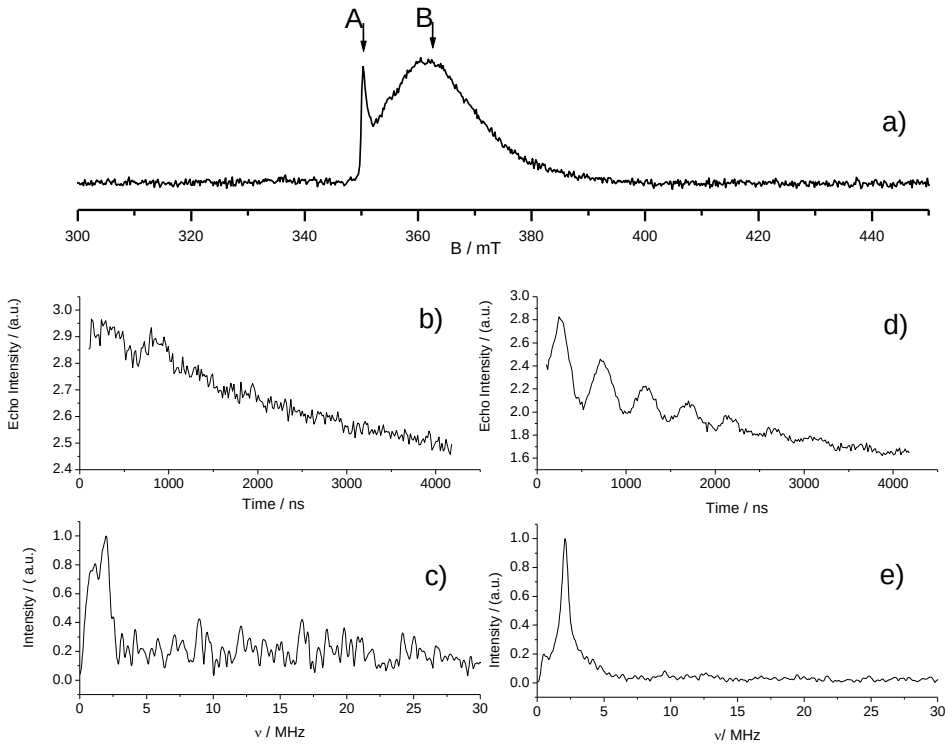

Figure 4. a) ESE detected EPR spectrum of ^{17}O enriched anatase UV irradiated under H_2; b) 3 pulse ESEEM spectrum taken at observer position A; c) corresponding frequency domain spectrum; d) 3 pulse ESEEM

spectrum taken at observer position B; e) corresponding frequency domain spectrum. All spectra were taken at 10 K.

3. 3 Reduced states by annealing under vacuo.

It is well established that titanium dioxide is a reducible oxide whose composition depends on the pressure of oxygen in the atmosphere. In particular molecular oxygen is released upon annealing the solid under *vacuo* leaving excess electrons in the (reduced) solid (Equation 1). While it is quite common to find in the literature EPR spectra observed after a substantial reduction by annealing (which display very broad and unstructured signals) it is infrequent to see reports on the effect of tiny reduction of the solid using this approach.

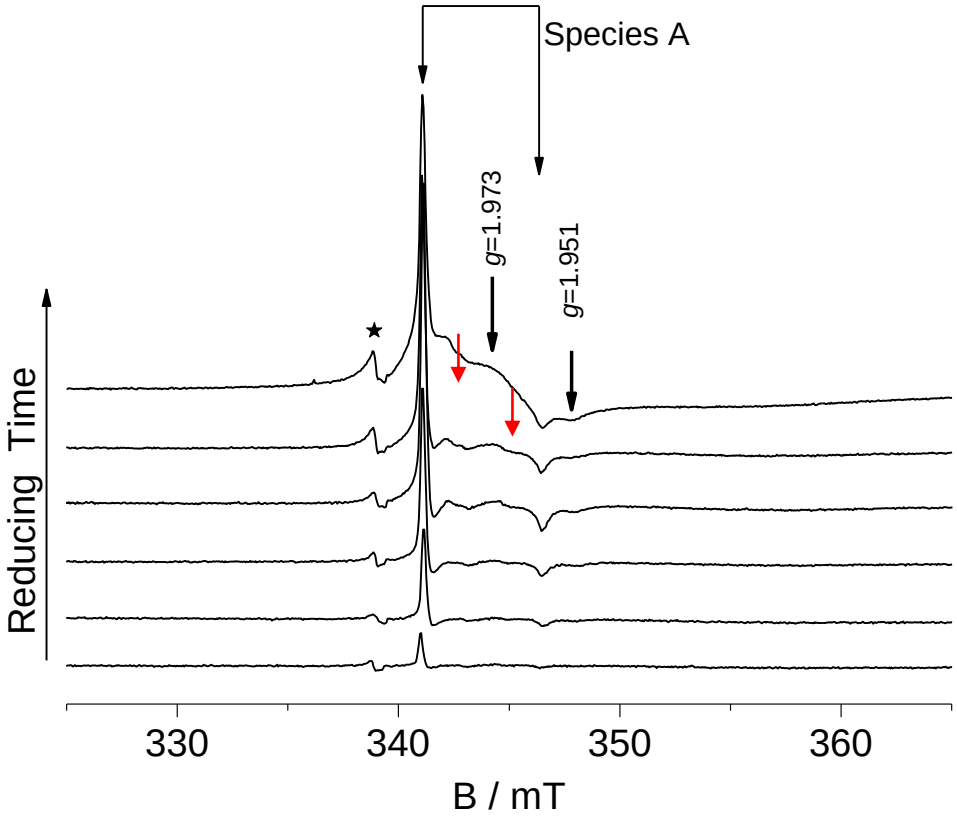

Fig 5. X-band CW-EPR spectra recorded at 77K of TiO_2 (anatase) prepared by CVD and submitted to a progressive annealing at 470K till a time of 3 hours (last spectrum).The two arrows indicate the features of species C.

Figure 5 shows the effect of a progressive reduction by annealing in rather mild conditions (470K) on the EPR spectra. The figure clearly shows that, in the early stages of the reduction, species A is practically the unique species observed whose intensity growths with increasing the annealing time. In the following stages of the treatment the signal of species A becomes perturbed by two other signals. The first one exhibits some weak feature in the spectral region covered by species A and results quite overlapped and thus incompletely resolved. A partial tentative assignment is illustrated by the arrows in Fig 5g suggesting the presence of *g* components of the new species (species C) at g = 1.951 and g= 1.973 The second species is the same broad and unstructured species (species B) already reported in Fig. 4 and assigned to surface titanium reduced species. The intensity of this third species is barely visible in the first spectra of the series due to its large linewidth but becomes much more appreciable, even in the CW spectrum, in the last spectra of the series. The star indicated a signal (g=2.003) ubiquitously present in reduced TiO_2 and usually associated to conduction band medium polarized electrons[41]. On the basis of the results reported in Fig. 5 it can be inferred that, after the very initial steps of oxygen depletion from the solid which involve reduction of lattice titanium ions, the dominant process is the reduction of the surface entailing the formation of a disordered partially reduced layer containing Ti^{3+} ions. The result of the reduction by annealing is not therefore very different, in qualitative terms from that described in Fig. 4 and obtained by interaction with reducing agents. If annealing of the solid is performed at progressively increasing temperature (Fig. 6) the result is quite similar to that reported in Fig. 5 except for the fact that the three Ti^{3+} species individuated so far are present since the first annealing of 30 minutes at 570K. At high annealing temperatures signal B becomes progressively dominant in the EPR spectrum. In the last spectrum obtained after reduction at 770K, in fact, species A is probably buried in the main signal or, alternatively, the disordered, defect-rich phase corresponding to signal B has expanded to encompass the subsurface region where species A was present (Fig. 6d). It is worth noticing that in such a conditions the anatase sample is coloured (pale grey-blue) and that the tuning of the resonant cavity prior to EPR spectra recording becomes difficult due to the decrease of the Q-factor of the cavity. This is due to the presence of conduction electrons in the materials.

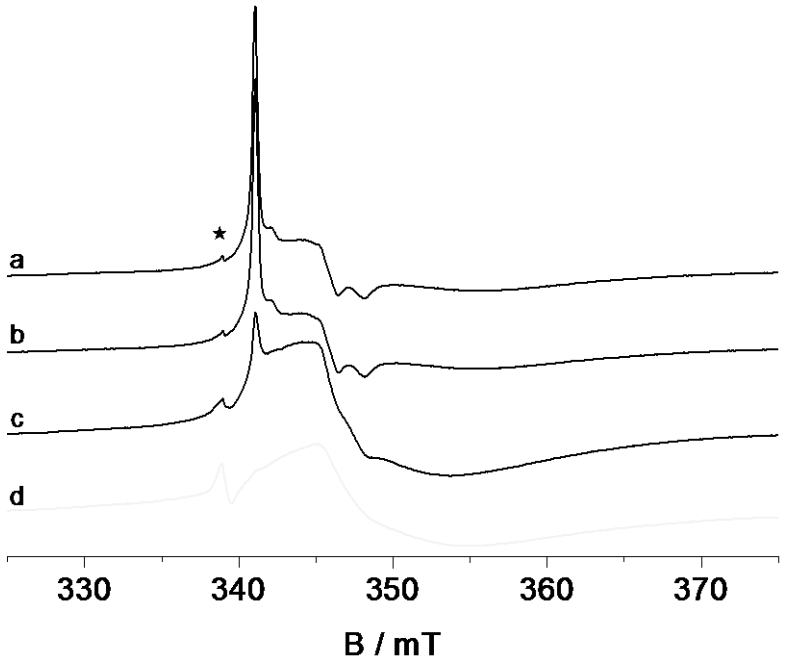

Fig 6. X-band CW-EPR spectra recorded at 77K of a TiO_2 (anatase) sample submitted to annealing at increasing temperature. a) 570K, 15 min; b) 570K, 30 min; c) 670K, 15 min; d) 770, 15min.

Species B is therefore observed in the case of both surface reaction with reducing agents and thermal annealing causing oxygen depletion.

3.4. Nature of the reduced Ti^{3+} centers.

The narrow, axial EPR signal labelled A in previous Sections has been observed several times in the past mainly in anatase under irradiation [16, 17, 21f,h] or in doped anatase[21g, 32, 33] and has been assigned either to Ti^{3+} in regular lattice sites[21g] or to the same ion in interstitial sites[16, 33], in all case without a firm and convincing evidence to support the assignment. As already anticipated in Section 3.1, we think that there is now a substantial bulk of evidence to propose the assignment of the axial signal with components $g_{\parallel}$ =1.962 and $g_{\perp}$=1.992 to a Ti^{3+} ion located in the regular, octahedrally coordinated site of the anatase lattice. This assignment is supported by a series of convincing evidences which are resumed in the following:

a) the signal is observed in different types of doped materials all containing excess electrons. The reported spectra of these materials are all recorded for fully oxidized samples. Since interstitial ions are often associated to crystals seriously disordered by thermal annealing

with consequent formation of oxygen vacancies, it is easy to note that all spectra reported in Fig. 1 related to differently doped materials and containing uniquely signal A are related to fully oxidized, undamaged materials. In all these case the presence of interstitial ions due to the structural perturbation consequent to oxygen loss can be excluded. A possible objection to this considerations could be based on the presence, also on fully oxidized materials, of a fraction of Ti^{4+} ions located in interstitial position and possible traps for excess electrons. This must correspond to the presence of Frankel defects (Ti vacancy + interstitial Ti) whose energetic cost, however, is extremely high (more than 19eV[42]) and strongly limits the formation of such centers. This consideration supports therefore our assignment.

b) The symmetry of the signal is strictly axial and even at high frequency (Fig. 1c) no resolution is observed between g_{xx} and g_{yy} thus indicating a corresponding symmetry of the Ti^{3+} coordination sphere. In the anatase matrix each titanium ion is surrounded by an axially elongated octahedron of oxygen ions. This symmetry is compatible with that of signal A. The situation is different in the case of the interstitial site. The nature of the interstitial sites in anatase is, in fact, rather different from that found in rutile. In rutile the interstitial site has indeed a symmetry comparable to that of the regular lattice site while in anatase an hypothetical interstitial titanium ion is in a low-symmetry quasi pyramidal environment [43] incompatible with the axial symmetry of the *g* tensor.

c) Theoretical calculations on large anatase supercells where one oxygen atom has been substituted with a fluorine one, point to the spontaneous formation of lattice Ti^{3+} ions as a consequence of fluorine insertion into the lattice[36] and have been confirmed by the group of G. Pacchioni[15c] in a recent comparative analysis of titania reduced in various ways.

This conclusive assignment of signal A has important implications in the general description of the behaviour of anatase as it indicates that, whatever the perturbation leading to excess electrons in the solid, the process starts with an initial reduction of the regular sites of the lattice (Fig.s 3, 5 and 6).

The features of signal B have been already discussed in a previous paragraph. This broad and featureless signal escapes to a detailed definition and it can be assumed that it reflect the complex situation occurring in the surface and subsurface region after a relatively abundant oxygen loss which has generated a disordered substoichiometric phase containing oxygen vacancies, reduced Titanium centres in various coordination states, itinerant electrons and so on. Since the idea that a reduced titanium ion could commonly occupy an interstitial position is quite widespread into the scientific community we have to say that the presence among the species contributing to signal B of interstitial Ti^{3+} ions cannot certainly be excluded. The fact

remains that the most clear evidence of interstitial Ti^{3+} have been found in rutile[21] while an unambiguous evidence of such a species in anatase is not yet available. The complexity of the described anatase reduced phases is hard to explore using polycrystalline solids but needs to be investigated with an approach typical of surface science using single crystals exposing a well defined face as in part done only in the case of rutile[44].

Similar considerations can be made for signal C which, though with better defined parameters, appears with signal B during the complex phase of the reduction of the solid. In this case further work is needed using advanced EPR techniques to understand the nature of this signal.

3.5 *Electron spin density and reduced lattice centres.*

As mentioned in the introduction the state of excess electrons in titanium dioxide in particular in terms of space distribution of the corresponding wave function is the object of an intense debate as this parameter is crucial for those applications of the oxide implying generation, dynamics and reactivity of charge carriers. EPR is certainly a suitable technique to describe the electron spin density around a given paramagnetic centre. This description, however, cannot be based on the *g* tensor alone but needs the measure of the electron-nucleus (or hyperfine) interaction occurring when nuclei with non zero nuclear spin constitutes the centre and/or its immediate surroundings. This is not the case of titanium dioxide in which the natural abundance of active nuclei is too low to permit observation of hyperfine structures. To overcome this problem our group has proposed, in the case of alkali earth oxides which have an analogous situation,[45] a method based on the introduction of ^{17}O into the oxide lattice via chemical procedures.

Very recently the ^{17}O hyperfine interaction around Ti^{3+} ions has been successfully monitored, in the case of a molecular compound (the esa-aquo complex $[Ti(H_2{}^{17}O)_6]^{3+}$)[46] and, following the approach here discussed, in that of the interstitial Ti^{3+} site in reduced "blue" rutile[47]. In both cases the small hyperfine interaction between the Ti unpaired electron and the oxygen nuclei was revealed using the HYSCORE (Hyperfine Sublevel Correlation) spectroscopy[48]. The observed ^{17}O couplings in these two cases are of the same order (maximum coupling of about 10MHz with a relatively large Fermi contact term of about 8 MHz) and can reasonably be assumed as reference values for slightly distorted $Ti^{3+}O_6$ systems having a localized electron in the titanium *d* orbitals . The same procedure followed in the case of the Ti^{3+} centres in the Blue rutile [47] is here adopted to study the hyperfine features of signal A in a F doped anatase sample. ^{17}O oxygen enrichment of the anatase matrix was obtained employing, during the hydrolysis, ^{17}O enriched water, leading to a nominal isotopic content of 40% (see Section 2). The CW-EPR spectrum of the resulting F doped, ^{17}O enriched sample, is equal to the one previously described in section 3.1 for the non enriched material. This indicates that hyperfine interactions in the systems are undetectable via the ordinary CW technique.

For this reason, in order to probe the spatial extent of the unpaired electron wave function, HYSCORE spectra, have been recorded at different field positions corresponding to the principal *g* factors of the EPR spectrum. A typical spectrum is reported in Figure 7 and shows the presence of a small ridge appearing in the (+,+) quadrant with maximum extension of about 2 MHz and centered at the ^{17}O nuclear Larmor frequency. This signal clearly indicates the presence of weakly coupled ^{17}O with maximum coupling not exceeding 2 MHz. This result is distinctly different from what observed on a reduced rutile sample with the same nominal concentration of ^{17}O. In that case, in fact a distinct ^{17}O hyperfine interaction with maximum coupling of about 10 MHz was observed, which is absent in this case. The ^{17}O coupling observed for the blue rutile sample is analogous to that observed in the Ti^{3+} esaquo molecular complex and indicates a degree of localization of the unpaired electron wave function similar in the two cases. The result reported in the case of the F doped anatase sample indicates a very different situation, whereby no resemblance to the molecular analog can be found. The absence of a distinct ^{17}O coupling suggests thus that in the case of the F doped anatase, the unpaired electron wave functions samples a larger number of oxide anions indicating a more delocalized nature of the defect.

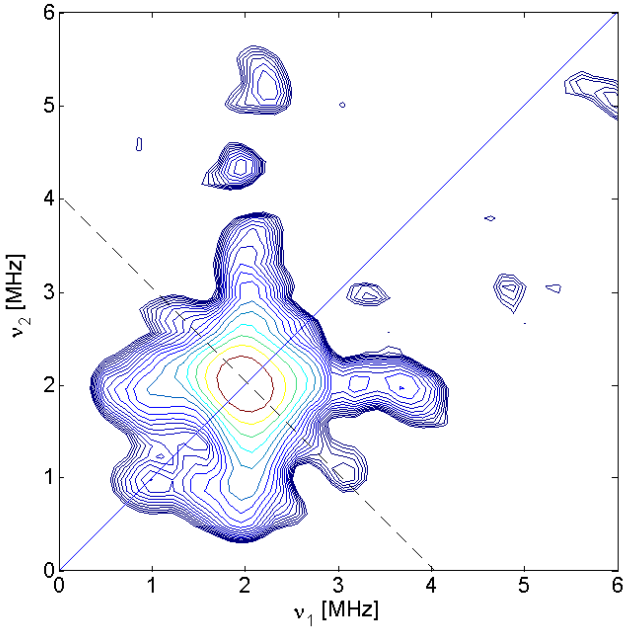

Figure 7. ^{17}O HYSCORE spectrum of F doped anatase recorded at an observer position corresponding to the $g_{\perp}$ component of the EPR spectrum (position A in figure 3c).The spectrum was recorded at 4 K.

It has to be recalled again that the systematic theoretical analysis of TiO_2 containing excess electrons performed by Pacchioni's group[15c] led, in the case of F-doped and Nb-doped anatase, to the result of two opposite solutions (excess electron fully localized in a d_{xy} orbital and delocalized electron) having practically the same total energy.

The data here reported have the limit of not providing an exact measure of the (too small) ^{17}O hyperfine interaction associated to lattice Ti^{3+} ions in anatase (signal A). They are however sufficient to exclude, for the interpretation of the centre corresponding to signal A, two limiting situations namely that of a wavefunction fully localized on a single titanium d orbital (similarly to what found for the interstitial species in "blue" rutile) and that corresponding to a free electron in the conduction band which should have completely different lineshape and relaxation parameters. The most probable situation is that corresponding to an electron delocalization over a discrete number of lattice sites with a wavefunction maintaining the typical axial symmetry clearly indicated by the *g* tensor. This picture corresponds to that of the so called large polaron which have been described in the lattice of several semiconducting systems[49]

4. Conclusions

The joint use of classic CW-EPR with pulsed EPR has led us to new insights into the properties of excess electrons in titanium dioxide (anatase polymorph). The main findings of the present work can be resumed as follows.

a. Three main EPR signals are observed when excess electrons are present in the solid. Signal B (centered at g=1.93) is broad and unfeatured and is the fingerprint of an extended reductive process which, as shown by ESEEM, involves the external layers of the microcrystals. The heterogeneity typical of this situation (various crystal faces, Ti^{3+} in different coordination, presence of oxygen vacancies) is reflected by the substantial *g* strain which is responsible of the large signal linewidth. Signal B is very similar in both chemically reduced (Fig.2) and thermally reduced materials (Fig.3) suggesting that also in this latter case some oxygen ion is removed by the action of the reducing agent. Signal C is a minor one and appears after prolonged reduction. The partial overlap with signal B hampers a deeper analysis of its features.

b. Signal A (axial and narrow, $g_{\|}$=1.962, $g_{\perp}$= 1.992) is conclusively assigned to Ti^{3+} ions in regular position of the anatase lattice. They form when electrons are introduced in the system by valence induction (Fluorine or Niobium doping) or in the early stages of reductive process obtained either by reaction with reducing agents or by thermal depletion of oxygen. The study of the hyperfine interaction between the Ti^{3+} unpaired electron and the

surrounding oxygen ions for this center has been performed for the first time introducing ^{17}O into the solid. This has allowed to and to evaluate the extent of the hyperfine interaction in the case of signal A which does not correspond to an individual species with a full localization of the excess electron into a d orbital of the ion but, much likely, to a species based on the delocalization of the electrons in the d orbitals of a number of structurally analogous lattice ions similar to that of a large polaron. An evaluation of the number of lattice Ti^{3+} ions actually involved in the electron wavefunction is not possible on the basis of the present data and should become possible only when data on titanium hyperfine constants will also become available. This result (compatible with recent theoretical calculations[15]) together with that concerning the reduced rutile phase[47] contributes to the debate about localisation and delocalisation of electrons in titania which is strategic for a variety of phenomena concerning the behaviour of charge carriers in this oxide.

Acknowledgments

We gratefully acknowledge long and fruitful discussions with Gianfranco Pacchioni and Cristiana di Valentin (Università di Milano Bicocca). We are grateful to Maria Fittipaldi (University of Florence) for measuring the W band spectrum. We also thanks the "Fondazione Cariplo" (Milano) for financial support to this research.

We whish to dedicate this paper to prof. Cesare Pisani, leader of the Theoretical Chemistry Group in our University and close friend of us who passed away on the 24th of July 2011.

References

(1) Linsebigler A.L; Lu G.Q.; Yates J. T. *Chem Rev*. **1995**, *95*, 735-758.
(2) *Photocatalysis: Fundamentals and Applications*; Serpone, N.; Pelizzetti, E, Eds; Wiley & Sons: Chicister, **1989**
(3) Honda, K.; Fujishima A. *Nature* **1972**, *238*, 37-38.
(4) Cho, M.; Chung, H.; Choi, W.; Yoon, J. Water Research **2004**, *38*, 1069-1077.
(5) Nozawa, M.; Tanigawa, K.; Hosomi, M.; Chikusa, T.; Kawada, E. *Water Science and Technology* 44 (9), pp. 127-133
(6) Watanabe, T.; Nakajima, A.; Wang, R.; Minabe, M.; Koizumi, S.; Fujishima, A.; Hashimoto, K. Thin Solid Films **1999**, *351*, 260-263.
(7) Hagfelt, A.; Grätzel, M. *Chem. Rev*. **1995**, ***95***, 49-68.
(8) Thompson, T. L.; Yates, J. T. *Chem. Rev*. **2006**, *106*, 4428-4453.
(9) Chen, X.; Mao, S. S. *Chem Rev*. **2007**, 107, 2881-2959.
(10) Chiesa, M.; Paganini, C.; Giamello, E. *Appl. Mag. Res*. **2010**, *37*, 605-618.
(11) Diebold, U. *Surf. Sci. Rep*. **2003**, *48*, 53-229.
(12) Tasker, P.W. *J. Phys. C* **1979**, 12**,** 4977-4984.
(13) Lafemina, J. P. Crit. Rev. Surf. Chem. **1994**, *3*, 297-332.
(14) a) Deskins, N.A.; Dupuis M. J. Phys. Chem. C **2009**, *113*, 346-358; b) Deskins, N. A. ; Rousseau, R.; Dupuis, M. J. Phys. Chem. C **2010**, *114*, 5891-5897.

(15) a) Di Valentin, C.; Pacchioni, G.; Selloni, A. *Phys. Rev. Lett.* **2006**, *97*, 166803 ; b) Finazzi, E.; Di Valentin, C.; Pacchioni, G. J. Phys. Chem. C **2009**, *113*, 3382-3385; c) Di Valentin, C.; Pacchioni, G.; Selloni, A. J. Phys. Chem. C **2009**, *113*, 20543-20552.
(16) Howe, R.F.; Gräztel, M. *J. Phys. Chem.*, **1985**, *89*, 4495-4499.
(17) Howe, R.F.; Gräztel, M. *J. Phys. Chem.*, **1987**, *91*, 3906-3909.
(18) Kurtz, R.L.; Stock-Bauer, R.; Madey, T. E. *Surf. Sci.* **1989**, *218*, 178-200.
(19) Khomenko, V.M.; Langer, K.; Rager, H.; Fett, A. *Phys. Chem. Miner.* **1998**, *25*, 338-346.
(20) Henderson, M.A.; Epling, W.S.; Peden, C.H.F.; Perkins, C. L. *J. Phys. Chem. B* **2003,** *107*, 534-545.
(21) a) Aono, M.; Hasiguti, R. R. *Phys Rev. B*, **1993**, *48*, 12406-12414; b) Berger,T.; Sterrer, M., Diwald, O.; Knozinger, E. *J. Phys.Chem. B*, **2005**, *109*, 6061-6068; c) Li, M.; Hebenstreit, W.; Diebold, U.; Tyryshkin, A. M.; Bowman, M. K.; Dunham, G. G.; Henderson, M. A. *J. Phys. Chem. B* **2000**, *104*, 4944-4950; d) Attwood, A.L.; Murphy, D.M.; Edwards, J.L.; Egerton, T.A.; Harrison, R.W. *Res. Chem. Intermediates*, **2003**, *29*, 449-465; e) Hurum, D.C.; Gray, K.A. *J. Phys. Chem. B*, **2005**, *109*, 977-980; f) Coronado, J.M.; Maira, A.J.; Conesa, J.C.; Yeung, K.L.; Augugliaro, V.; Soria, J. *Langmuir*, **2001**, *17*, 5368-5374; g) Meriaudau, P.; Che, M.; Jørgensen, C.K. Chem. Phys. Lett. **1970**, 5, 131-133; h) Micic, O.I.; Zhang, Y.N.; Cromack, K.R.; Trifunac, A.D.; Thurnauer, M.C. *J. Phys. Chem. B*, **1993**, *97*, 7277-7283.
(22) Wendt, S.; Sprunger, P. T.; Lira, E.; Madsen, G. K. H. M.; Li, Z.;Hansen, J.; Matthiensen, J.; Blekinge-Rasmussen, A.; Lægsgaard, E.;Hammer, B.; Besenbacher, F. *Science* **2008**, *320*, 1755-1759.
(23) Kruger, P.; Bourgeois, S.; Domenichini, B.; Magnan, H.; Chandesris, D.; Le Fevre, P.; Flank, A. M.; Jupille, J.; Floreano, L.; Cossaro, A.;Verdini, A.; Morgante, A. *Phys. Rev. Lett.* **2008**, *100*, 055501.
(24) Deskins N.A.;Dupuis, M. *Phys. Rev. B* **2007**, *75*, 195212.
(25) Chiesa, M.; Giamello E. *"Electron Paramagnetic Resonance of Charge Carriers in Solids"* in M. Brustolon and E. Giamello Ed.s *Electron Paramagnetic Resonance: a practitioner's toolkit* Wiley 2010
(26) Zimmermann, P.H. *Phys. Rev. B* **1973**, *8*, 3917-3927.
(27) Yang, S.; Halliburton, L.E.; Manivannan, A.; Bunton, P. H.; Baker, D. B.; Kemm, M.; Horn, S.; Fujishima A. A*ppl. Phys. Lett* **2009**, *94*, 162114.
(28) Yang, S.; Halliburton L. E.; *Phys. Rev. B* **2010**, 81, 035204.
(29) Knözinger, E.; Diwald, O.; Sterrer, M. *J. Mol. Catal. A: Chemical* **2000**, *162*, 83–95.
[30] P. Höfer, A. Grupp, H. Nebenführ, M. Mehring, *Chem. Phys. Lett.* **1986**, *132*, 279.
[31] S. Stoll,.; A. Schweiger, *J. Magn. Reson*. **2006**, *178*, 42.
(32) Valigi, M.; Cordischi, D.; Minelli, G.; Natale, P.; Porta, P.; Kreijzers, C.P. *J. Solid State Chem.* **1988**, *77, 255-263.*
(33) Kiwi, J.; Suss, J. T.; Zsapiro S. *Chem Phys. Lett.* **1984**, 106, 135-138.
(34) Yu, J. C.; Yu, J.; Ho, W.; Jiang, Z.; Zhang, L. *Chem. Mater.* **2002**, *14*, 3808-3816.
(35) Li, D.; Haneda, H.; Labhsetwar, N.; Hishita, S.; Ohashi, N. *Chem. Phys. Lett.* **2005**, *401*, 579-584.
(36) Czoska, A. M.; Livraghi, S.; Chiesa, M.; Giamello, E.; Finazzi, E.; Di Valentin, C.; Pacchioni, G.; Agnoli, S.; Granozzi, G. *J. Phys. Chem. C* **2008**, *112*, 8951-8956.
(37) Berger, T.; Diwald, O.; Knoezinger, E.; Napoli, F.; Chiesa, M.; Giamello E. Chem. Phys. **2007**, *339*, 138-145.
(38) Livraghi, S.; Olivero, F.; Paganini, M. C.; Giamello E. *J. Phys. Chem. C* **2010**, *114*, 18553-18558.
(39) Pan, J. M.; Maschhoff, B. L.; Diebold, U.; Madey, T. E. *J. Vac. Sci. technol. A* **1992,** *10*, 2470-2476.
(40) Henderson, M.A.; Epling, W.S.; Perkins, C.L.; Peden, C.H.F.; Diebold, U. *J. Phys. Chem. B* **1999**, *103*, 5328-5337.
(41) Serwicka, E.; Schlierkamp, M.W.; Schindler, R.N. *Z. Naturforsch* **1981**, *36a*, 226-232.
(42) Olson, C.; Nelson, J.; Saiful Islam M. *J. Phys. Chem. B 1996, 110*, 9995-10001.
(43) Finazzi, E.; Di Valentin, C.; Pacchioni G. *J. Phys. Chem. C* **2009**, *113*, 3382-3385.
(44) a) Henderson M.A. *Surf. Sci* **1995**, *343*, L1156-L1160, b) Henderson M.A. *Surf. Sci* **1999**, *419*, 174-187.
(45) a) Chiesa, M.; Martino, P.; Giamello, E.; Di Valentin, C.; Del Vitto, A.; Pacchioni. G. *J. Phys. Chem. B* **2004**,*108*, 11529-11534, b) Chiesa, M.; Giamello, E.; Di Valentin, C.; Pacchioni. G. *Chem. Phys. Lett.* **2005**, *43*, 124-128, c) Chiesa, M.; Paganini, M.C.; Giamello, E.; Di Valentin, C.; Pacchioni, G. *Chemphyschem* **2006**, *7*, 728-734, Chiesa, M.; Paganini, M. C.; Giamello, E.; Murphy, D. M.; Di Valentin, C.; Pacchioni, G. *Acc. Chem. Res.* **2006**, 39, 861-867.
(46) Maurelli, S.; Livraghi, S.; Chiesa, M.; Giamello, E.; Van Doorslaer, S.; Di Valentin, C.; Pacchioni, G. *Inorg. Chem.* **2011**, *50*, 2385-2394.
(47) Livraghi, S.; Maurelli, S.; Paganini, M.C.; Chiesa, M.; Giamello E. *Angew. Chem. Int. Ed.* **2011**, *50*, 8038-8040.
(48) Höfer, P.; Grupp, A.; Nebenführ, H.; Mehring, M. *Chem. Phys. Lett.* **1986**, *132*, 279-282.
(49) Stoneham A. M., Gavartin, J; Shluger, A. L.; Kimmel, A. V.; Muñoz Ramo, D.; Rønnow, H. M.; Aeppli, G.; Renner, C. *J. Phys.: Condens. Matter* **19** 255208.

Graphical Abstract

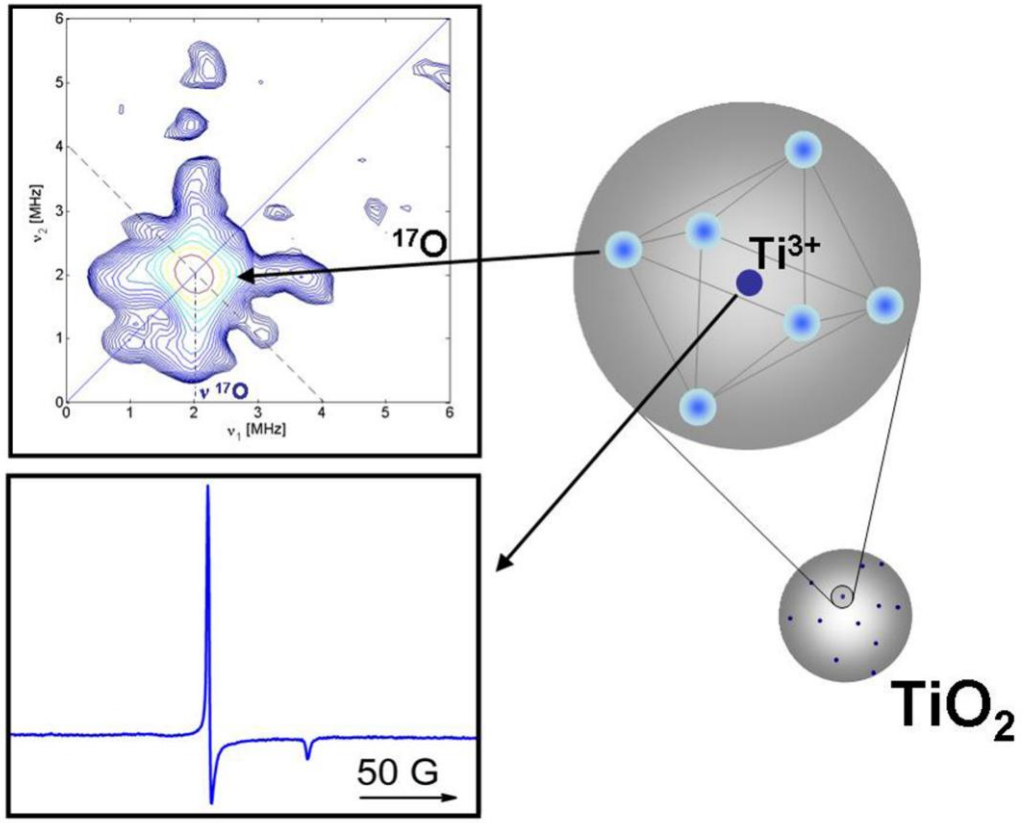
^{17}O
$\nu_{^{17}O}$
ν_2 [MHz]
ν_1 [MHz]
Ti^{3+}
50 G
TiO_2